HHS Public Access

Author manuscript

Neurotoxicology. Author manuscript; available in PMC 2018 September 01.

Published in final edited form as:

Neurotoxicology. 2017 September ; 62: 200–206. doi:10.1016/j.neuro.2017.07.028.

Methylmercury augments Nrf2 activity by downregulation of the Src family kinase Fyn

Megan Culbreth, **Ziyan Zhang**, and **Michael Aschner**

Department of Molecular Pharmacology, Albert Einstein College of Medicine, Bronx, NY

Abstract

Methylmercury (MeHg) is a potent developmental neurotoxicant that induces an oxidative stress response in the brain. It has been demonstrated that MeHg exposure increases nuclear factor erythroid 2-related factor 2 (Nrf2) activity. Nrf2 is a transcription factor that translocates to the nucleus in response to oxidative stress, and upregulates phase II detoxifying enzymes. Although, Nrf2 activity is augmented subsequent to MeHg exposure, it has yet to be established whether Nrf2 moves into the nucleus as a result. Furthermore, the potential effect MeHg might have on the non-receptor tyrosine kinase, Fyn, has not been addressed. Fyn phosphorylates Nrf2 in the nucleus, resulting in its inactivation, and consequent downregulation of the oxidative stress response. Here, we observe Nrf2 translocates to the nucleus subsequent to MeHg-induced oxidative stress. This response is concomitant with reduced Fyn expression and nuclear localization. Moreover, we detected an increase in phosphorylated Akt and glycogen synthase kinase 3 beta (GSK-3β) at activating and inhibitory sites, respectively. Akt phosphorylates and inhibits GSK-3β, which subsequently prevents Fyn phosphorylation to signal nuclear import. Our results demonstrate MeHg downregulates Fyn to maintain Nrf2 activity, and further illuminate a potential mechanism by which MeHg elicits neurotoxicity.

Keywords

methylmercury; Nrf2; Fyn; oxidative stress

Introduction

Methylmercury (MeHg) is an established developmental neurotoxicant. It is particularly detrimental to the nervous system consequent to high-dose *in utero* exposure (Bakir et al. 1973; Harada 1995). It remains unclear, however, at what threshold concentration MeHg becomes developmentally neurotoxic. Furthermore, epidemiological studies have been inconclusive about the developmental impact of gestational MeHg exposure in populations, which consume fish, the primary exposure route in humans, as a dietary staple (Davidson et

Corresponding Author: Megan Culbreth, 1300 Morris Park Ave., Forchheimer 206, Bronx, NY 10461, (718) 839-7920, megan.culbreth@phd.einstein.yu.edu.

al. 2008; Davidson et al. 2011; Debes et al. 2006; Grandjean et al. 1997). Reports in animal models document increased brain mercury (Hg) concentration in neonates exposed *in utero* (Newland and Reile 1999). Moreover, enhanced Hg deposition in cortical astrocytes has been observed (Charleston et al. 1995). Despite extensive research, however, the mechanism(s) by which MeHg elicits neurotoxicity are not fully elucidated.

It is well known MeHg induces oxidative stress in the brain. Exposure enhances reactive oxygen species (ROS) generation (Shanker et al. 2004) and lipid peroxidation (Yin et al. 2007). Furthermore, MeHg inhibits glutathione peroxidase (Franco et al. 2009), an enzyme involved in ROS detoxification. Nonetheless, a direct correlation between oxidative stress induction and resultant toxicity is ambiguous. Nuclear factor erythroid 2-related factor 2 (Nrf2), a transcription factor, has potential to clarify this connection. Nrf2 translocates to the nucleus in response to oxidative stress, and promotes transcription of phase II detoxifying enzymes (Itoh et al. 1997). It has been demonstrated that MeHg increases total Nrf2 protein and upregulates antioxidant gene transcription (Ni et al. 2011). Although Nrf2 activity is enhanced subsequent to MeHg exposure, it has yet to be determined whether Nrf2 translocates to the nucleus as a consequence.

Additionally, the potential impact MeHg exposure has on the Src family kinase, Fyn, has not been explored. Nrf2 activation of phase II detoxifying enzyme transcription requires Fyn nuclear export (Kaspar and Jaiswal 2011). Moreover, Fyn phosphorylates Nrf2, signaling Nrf2 nuclear export, and subsequent downregulation of the oxidative stress response (Jain and Jaiswal 2006). Thus, the dynamic between Fyn and Nrf2 could provide vital insight into the mechanism of MeHg toxicity. It has been demonstrated that glycogen synthase kinase 3 beta (GSK-3β) phosphorylates Fyn, to signal nuclear import (Jain and Jaiswal 2007). However, GSK-3β and the signaling pathway, which regulates its activity, have not been examined consequent to MeHg exposure. Akt inactivates GSK-3β (Cross et al. 1995). Furthermore, it was previously shown that phosphoinositide 3-kinase (PI3K) inhibition reduces Nrf2 activity (L Wang et al. 2009). PI3K stimulates Akt activation (Franke et al. 1995). Therefore, we hypothesized MeHg downregulates Fyn via Akt/GSK-3β signaling, in order to sustain Nrf2 activation.

In the present study, we assessed Nrf2 subcellular localization subsequent to MeHg exposure at a time (6 hours) and concentration (5 μM), which elicit maximal Nrf2 activation in primary cortical astrocytes. Furthermore, we examined Fyn expression and localization, as well as the signaling pathway, which precedes its nuclear import. Our results suggest MeHg downregulates Fyn as to maintain Nrf2 activity.

Materials and Methods

Cell Culture

Primary astrocytes were isolated from postnatal day 1 Sprague-Dawley rats as previously described (Allen et al. 2001). Briefly cortices were separated, meninges removed, and dissociated with dispase. Cells were plated at 10,000 cells/cm^2 on poly-l-lysine coated dishes, and maintained in minimum essential medium (MEM) supplemented with 10% horse serum. After 1–2 weeks in culture, astrocytes were used for respective experiments.

Chemicals

Methylmercury chloride (MeHg) was purchased from Sigma-Aldrich (St. Louis, MO). Stock solutions were made in water (biotech grade) (Fisher) and stored at −20°C. For all experiments, stocks were diluted to a final concentration (5 μM) in MEM without phenol red supplemented with 1% horse serum. 5 μM MeHg was the lowest concentration at which a significant decrease in cell viability was observed (data not shown).

MTT Assay

Cell viability was assessed by 3-(4,5-dimethylthiazol-2-yl)-2,5-diphenyltetrazolium (MTT) cleavage. MTT was purchased from Thermo Scientific (Rockford, IL), a stock solution made in Hank's Balanced Salt Solution (HBSS), and stored at 4°C. Briefly, astrocytes cultured in 96-well plates were exposed to MeHg for 6 hours, treatment was removed, and cells were incubated with MTT. MTT was solubilized in dimethyl sulfoxide (DMSO) and absorbance measured at 570 nm. Background absorbance (690 nm) was subtracted from results.

LDH Assay

Cytotoxicity was measured by lactate dehydrogenase (LDH) release using the Pierce LDH Cytotoxicity Assay Kit (Thermo Scientific) according to manufacture instructions. Briefly, astrocytes cultured in 96-well plates were exposed to MeHg for 6 hours, supernatant transferred to a new plate, and incubated with reaction mixture. LDH absorbance was measured at 490 nm. Background absorbance (690 nm) was subtracted from results.

ROS Generation

Reactive oxygen species (ROS) generation was assessed by CM-H2DCFDA (Invitrogen) fluorescence according to manufacture instructions. Briefly, astrocytes cultured in 96-well plates were pre-incubated with 5 μM CM-H2DCFDA for 20 min at 37°C, CM-H2DCFDA removed, and exposed to MeHg for 6 hours. Fluorescence was measured at 520 nm (excitation at 485 nm).

Quantitative Real-Time PCR

Total RNA was purified from astrocytes cultured in 60mm dishes with the RNeasy® Mini Kit (Qiagen), then reverse transcribed to cDNA with the High Capacity cDNA Reverse Transcription Kit (Thermo Scientific). Heme-oxygenase 1 (Hmox1), NAD(P)H quinone dehydrogenase 1 (Nqo1), and Fyn mRNA expression were measured by quantitative realtime PCR (qRT-PCR) using TaqMan® Gene Expression Assay probes (Thermo Scientific). The comparative $2^{-\Delta\Delta Ct}$ method (Livak and Schmittgen 2001) was used to determine fold difference, and normalized to glyceraldehyde 3-phosphate dehydrogenase (Gapdh). The following probes were used: Hmox1 (Assay ID: Rn00561387_m1), Nqo1 (Assay ID: Rn00566528_m1), Fyn (Assay ID: Rn00562616_m1), and Gapdh (Assay ID: Rn01775763_g1).

Immunocytochemistry

Astrocytes cultured on glass coverslips were fixed (4% paraformaldehyde), permeabilized (0.1% Triton), and blocked (5% bovine serum albumin). Cells were incubated overnight with

rabbit anti-Nrf2 (1:50) (Santa Cruz). Secondary antibody was Alexa Fluor® 488 goat-anti rabbit (1:500) (Thermo Scientific). Coverslips were mounted with ProLong™ Gold antifade reagent with DAPI.

Microscopy and Analysis

An Inverted Olympus IX81 Widefield Microscope (20X objective, NA = 0.40 Air, no boost) and Sensicam QE cooled CCD camera were used to capture fluorescent images. An image of a single area of interest was acquired in two fluorescent channels, Alexa 488 and DAPI, displayed, and measured in Volocity™ (Perkin Elmer Inc.). A protocol was established to measure the overlap of Nrf2 (stained with Alexa 488) and the nucleus of the cell (stained with DAPI). Briefly, cell nuclei were identified in the DAPI channel using average area to distinguish individual cells. The total cell area was then determined in the Alexa 488 channel. The intersect of Alexa 488 with DAPI was used to quantify Nrf2 nuclear intensity. Intensity is the average Nrf2 fluorescence as measured in pixels for a single cell. The mean intensity was used to compare untreated to treated. For each condition the identical protocol was applied.

Subcellular Fractionation

Cytoplasmic and nuclear fractions were isolated with NE-PER Nuclear and Cytoplasmic Extraction Reagents (Thermo Scientific) according to manufacture instructions. Briefly, astrocytes cultured in 100mm dishes were detached with phosphate buffered saline (PBS) plus protease inhibitor cocktail (Sigma), and cytoplasmic and nuclear fractions separated. Fractions were subjected to sodium dodecyl sulfate polyacrylamide gel electrophoresis (SDS-PAGE), and analyzed by western blot. Primary antibodies for rabbit anti-Nrf2 (1:1000) and rabbit anti-Fyn (1:1000) were purchased from Cell Signaling Technology (CST) (Danvers, MA). Mouse anti-α tubulin (CST) and rabbit anti-histone H3 (abcam) were used as cytosolic and nuclear loading controls, respectively. Secondary antibodies were goat anti-rabbit HRP and goat anti-mouse HRP (Thermo Scientific).

Whole-cell Protein Extraction

Astrocytes cultured in 60mm dishes were lysed with RIPA Buffer (Sigma) plus protease inhibitor cocktail to obtain whole-cell lysates. Lysates were subjected to SDS-PAGE, and analyzed by western blot. Primary antibodies for p-Akt (Thr308), Akt, p-GSK-3β (Ser9), and GSK-3β (1:1000) were purchased from CST; Sp1 was purchased from abcam. Mouse anti-β actin (Sigma) was used as loading control. Secondary antibodies were goat anti-rabbit HRP and goat anti-mouse HRP (Thermo Scientific).

Densitometry

ImageJ was used to quantify western blots from subcellular fractions and whole-cell lysates. Cytosolic fractions, nuclear fractions, and whole-cell lysates were normalized to α-tubulin, histone H3, and β-actin, respectively.

Statistical Analysis

All data are reported as mean ± standard error of the mean (SEM). Differences between treatments were analyzed by one-way analysis of variance (ANOVA), followed by Tukey's HSD *post-hoc* test using RStudio®. Statistical significance was set at $p < 0.05$.

Results

Astrocytes are vulnerable to MeHg-induced toxicity

Cell viability and cytotoxicity were determined by MTT and LDH assays, respectively. MTT assesses the number of live cells as a function of mitochondrial activity. We observed a significant decrease in cell viability (76.7 ± 6.7, $p < 0.05$; $n = 3$) as a result of MeHg exposure compared to untreated controls (Fig. 1A). LDH measures cell membrane integrity as a function of extracellular LDH release. We observed a significant increase in cytotoxicity (127.2 ± 3.9, $p < 0.001$; $n = 4$) as a result of MeHg exposure compared to untreated controls (Fig. 1B).

Methylmercury induces oxidative stress and Nrf2 activation

Oxidative stress was determined by CM-H2DCFDA fluorescence. CM-H2DCFDA is cleaved in the presence of oxidants, and creates a fluorescent by-product. We observed a significant increase in ROS generation (134.9 ± 3.0, $p < 0.001$; $n = 4$) as a result of MeHg exposure compared to untreated controls (Fig. 1C). Nrf2 transcriptional targets Hmox1 and Nqo1 were measured by qRT-PCR. We observed a significant increase in Hmox1 (108.6 ± 13.6, $p < 0.001$; $n = 5$) and Nqo1 (3.68 ± 0.4, $p < 0.001$; $n = 6$) expression as a result of MeHg exposure compared to untreated controls (Fig. 1D).

Nrf2 translocates to the nucleus in response to methylmercury exposure

Nrf2 localization was assessed by immunocytochemistry and subcellular fractionation. Immunostained astrocytes exhibited ubiquitous Nrf2 expression (Fig. 2A). We observed a significant increase in Nrf2 in cell nuclei (1.47 ± 0.08, $p < 0.01$; $n = 4$) as a result of MeHg exposure compared to untreated controls (Fig. 2A,B). We also detected a significant increase in Nrf2 in nuclear fractions (1.58 ± 0.10, $p < 0.01$; $n = 3$) as a result of MeHg exposure compared to untreated controls (Fig. 2C,D). However, there was no discernable change in Nrf2 in cytosolic fractions (0.97 ± 0.05, $p = 0.7$; $n = 3$) (Fig. 2C,E).

Methylmercury exposure downregulates Fyn

Fyn gene expression was analyzed by qRT-PCR. We observed a significant decrease (0.64 ± 0.07, $p < 0.001$; $n = 6$) as a result of MeHg exposure compared to untreated controls (Fig. 3A). Additionally, specificity protein 1 (Sp1), the transcription factor, which controls Fyn expression (Gao et al. 2009), was assessed by whole-cell western blot. We observed a significant decrease (0.56 ± 0.07, $p < 0.01$; $n = 3$) as a result of MeHg exposure compared to untreated controls (Fig. 3B,C). Fyn localization was also examined by subcellular fractionation. We detected a significant decrease in Fyn in nuclear fractions (0.62 ± 0.02, $p < 0.001$; $n = 3$) as a result of MeHg exposure compared to untreated controls (Fig. 3D,E). However, there was no discernable change in Fyn in cytosolic fractions (1.09 ± 0.09, $p = 0.4$;

n = 3) (Fig. 3D,F). Furthermore, we assessed the signaling cascade, which precedes Fyn nuclear import by whole-cell western blot. We observed a significant increase in p-Akt (2.25 ± 0.33, $p < 0.05$; n = 3) (Fig. 4A,B) and p-GSK-3β (1.63 ± 0.03, $p < 0.001$; n = 3) (Fig. 4A,C) as a result of MeHg exposure compared to untreated controls. There was no discernable change in total Akt (0.99 ± 0.04, $p = 0.7$; n = 3) or GSK-3β (1.00 ± 0.03, p = 1.0; n =3) (Fig. 4C).

Discussion

The pro-oxidative properties of MeHg have long been recognized (Fretham et al. 2012). MeHg enhances ROS generation two-fold: mitochondrial membrane potential decreases (Yin et al. 2007), which results in spurious electron escape from the electron transfer chain, and glutathione peroxidase activity is reduced (Franco et al. 2009), augmenting intracellular hydrogen peroxide (Shanker et al. 2004). These effects induce oxidative stress, which in turn upregulates antioxidant enzyme defenses directed by Nrf2 (L Wang et al. 2009). Nrf2 nuclear translocation is required to stimulate this response (Huang et al. 2000). It has not been quantifiably demonstrated, however, that MeHg promotes Nrf2 nuclear localization. Here, we confirm Nrf2 translocates to the nucleus consequent to MeHg exposure both by immunocytochemistry and subcellular fractionation. Furthermore, at the MeHg concentration and time-point examined, downstream antioxidant enzyme expression increases. Kelch-like ECH-associated protein 1 (Keap1) was also assessed to corroborate Nrf2 activation. Keap1 binds Nrf2 and represses its activity (Itoh et al. 1999). Moreover, it serves as an adaptor for ubiquitin ligases, which mark Nrf2 for proteasomal degradation (Kobayashi et al. 2004). We observed MeHg reduces Keap1 expression and protein level [Supp. Fig. 1].

To further elucidate the potential mechanism by which MeHg augments Nrf2 activity, we examined Fyn, a non-receptor tyrosine kinase, known to phosphorylate Nrf2 and signal its nuclear export (Jain and Jaiswal 2006). Fyn is also activated in response to oxidative stress (Abe and Berk 1999; Sanguinetti et al. 2003). Moreover, MeHg has been observed to increase Fyn kinase activity in oligodendrocyte precursor cells (Li et al. 2007). To our knowledge, however, a direct connection between Nrf2 and Fyn has not been examined consequent to MeHg exposure. Our study reveals, MeHg reduces Fyn transcription and Sp1, the transcription factor that regulates Fyn expression (Gao et al. 2009), total protein. Interestingly, Nrf2 was found to bind Sp1, and repress its activity at the Tgf-β1 promoter (Gao et al. 2014). We did observe a significant decrease in Tgf-β1 transcription (Supp. Fig. 2), however, additional experiments would be necessary to confirm Nrf2 binds Sp1 at the MeHg concentration and time-point examined.

In addition, Sp1 was observed to interact with Nrf2, and promote Hmox1 transcription (Chi et al. 2015). Intriguingly, Sp1 siRNA knockdown attenuated this response. Furthermore, this interaction was ROS-independent. Consequently, the detected Sp1 decrease reported herein could reveal a mechanism by which MeHg mitigates the antioxidant response apart from oxidative stress induction. We failed, however, to observe a concomitant decrease in Hmox1 expression. This potentially could be attributed to a compensatory mechanism. Several diverse signaling pathways regulate Hmox1 transcription (Kietzmann et al. 2003; Martin et

al. 2004; Pronk et al. 2014). p38 mitogen-activated protein kinase was previously demonstrated to induce Sp1-dependent Hmox1 activation (Lin et al. 2011). Moreover, Nrf2 translocation and activation are negatively regulated by p38 (Huang et al. 2000; Yu et al. 2000). Possibly, MeHg-induced Nrf2 activation downregulates p38/Sp1-dependent pathways, but this remains to be explored.

Nrf2 transcriptional activity requires Fyn nuclear export. Furthermore, the phosphorylation sites, which mediate this process are oxidant sensitive (Kaspar and Jaiswal 2011). It had yet to be investigated, however, whether MeHg has an effect on Fyn subcellular localization. Here, we observe a decrease in Fyn nuclear protein consequent to MeHg exposure. Interestingly, no change in Fyn cytosolic protein was detected. GSK-3β mediated Fyn phosphorylation is necessary for nuclear translocation (Jain and Jaiswal 2007). Moreover, this process is redox-sensitive. We detected an increase in GSK-3β serine 9 phosphorylation, subsequent to MeHg exposure. Akt phosphorylates GSK-3β at this site, inhibiting its activity (Cross et al. 1995). This result is inconsistent with a previous report, which found MeHg enhanced GSK-3β activity (Fujimura and Usuki 2015). However, the MeHg concentration examined was considerably lower than that in our report. In addition, the former study was in neural progenitor cells, likely more sensitive to MeHg-induced toxicity. We did not observe any change in active GSK-3β (Supp. Fig. 3). Other heavy metals have also been found to activate GSK-3β (DeFuria and Shea 2007; SH Wang et al. 2009). However, it remains to be determined whether the concentration, time-point, and model system employed contribute to this differential result.

PI3K/Akt have been shown to activate Fyn (Yadav and Denning 2011). However, this result was attributed to constitutively active Ras overexpression. To our knowledge, PI3K/Akt-induced Fyn activation has not been observed out of the oncogenic context. Interestingly, c-Src, another Src family non-receptor tyrosine kinase, was found to act upstream of PI3K/Akt in arachidonic acid (AA) stimulated Hmox1 transcription (Lin et al. 2017). Furthermore, PI3K/Akt induced extracellular-signal related kinase (Erk1/2) activation, and subsequent Nrf2 nuclear translocation. MeHg has been observed to enhance AA release (Shanker et al. 2002). Moreover, Erk1/2 phosphorylation increases at the same MeHg concentration and time-point (Yin et al. 2011) as examined in the present study. Here, we detected an increase in Akt threonine 308 phosphorylation, consequent to MeHg exposure. Phosphoinositide-dependent kinase-1 [PDK1] phosphorylates Akt at this site, potentiating its activity (Alessi et al. 1997). Our studies, for the first time, identify a plausible feedback loop, which sustains MeHg-induced Nrf2 activation (Fig. 5).

In summary, we have demonstrated MeHg-induces Nrf2 nuclear localization and subsequent upregulation of the phase II detoxifying enzyme response. Nrf2 activity is protracted by Fyn nuclear export, directed by Akt-stimulated GSK-3β inhibition. Furthermore, Sp1 regulated Fyn expression is reduced. Further studies, however, would be necessary to definitively determine how MeHg modulates this complex signaling cascade in order to elicit neurotoxicity over time.

Supplementary Material

Refer to Web version on PubMed Central for supplementary material.

Acknowledgments

The authors would like to acknowledge the Analytical Imaging Facility at Albert Einstein College of Medicine, particularly Hillary Guzik, for her support in developing the image analysis protocol. This work was funded by the National Institute of Health grants NIEHS R01ES07331 and NIEHS R01ES020852.

Abbreviations

MeHg	methylmercury
GSK-3β	glycogen synthase kinase 3 beta
ROS	reactive oxygen species
Nrf2	nuclear factor erythroid 2-related factor 2
ARE	antioxidant response element
Hmox1	heme oxygenase
Nqo1	NAD(P)H quinone dehydrogenase
Sp1	specificity protein 1

References

Abe J, Berk BC. Fyn and jak2 mediate ras activation by reactive oxygen species. J Biol Chem. 1999; 274:21003–21010. [PubMed: 10409649]

Alessi DR, James SR, Downes CP, Holmes AB, Gaffney PR, Reese CB, et al. Characterization of a 3-phosphoinositide-dependent protein kinase which phosphorylates and activates protein kinase balpha. Curr Biol. 1997; 7:261–269. [PubMed: 9094314]

Allen JW, Mutkus LA, Aschner M. Isolation of neonatal rat cortical astrocytes for primary cultures. Curr Protoc Toxicol Chapter. 2001; 12 Unit12 14.

Bakir F, Damluji SF, Amin-Zaki L, Murtadha M, Khalidi A, al-Rawi NY, et al. Methylmercury poisoning in iraq. Science. 1973; 181:230–241. [PubMed: 4719063]

Charleston JS, Body RL, Mottet NK, Vahter ME, Burbacher TM. Autometallographic determination of inorganic mercury distribution in the cortex of the calcarine sulcus of the monkey macaca fascicularis following long-term subclinical exposure to methylmercury and mercuric chloride. Toxicol Appl Pharmacol. 1995; 132:325–333. [PubMed: 7785060]

Chi PL, Lin CC, Chen YW, Hsiao LD, Yang CM. Co induces nrf2-dependent heme oxygenase-1 transcription by cooperating with sp1 and c-jun in rat brain astrocytes. Mol Neurobiol. 2015; 52:277–292. [PubMed: 25148934]

Cross DA, Alessi DR, Cohen P, Andjelkovich M, Hemmings BA. Inhibition of glycogen synthase kinase-3 by insulin mediated by protein kinase b. Nature. 1995; 378:785–789. [PubMed: 8524413]

Davidson PW, Jean Sloane R, Myers GJ, Hansen ON, Huang LS, Georger LA, et al. Association between prenatal exposure to methylmercury and visuospatial ability at 10.7 years in the seychelles child development study. Neurotoxicology. 2008; 29:453–459. [PubMed: 18400302]

Davidson PW, Cory-Slechta DA, Thurston SW, Huang LS, Shamlaye CF, Gunzler D, et al. Fish consumption and prenatal methylmercury exposure: Cognitive and behavioral outcomes in the main cohort at 17 years from the seychelles child development study. Neurotoxicology. 2011; 32:711–717. [PubMed: 21889535]

Debes F, Budtz-Jorgensen E, Weihe P, White RF, Grandjean P. Impact of prenatal methylmercury exposure on neurobehavioral function at age 14 years. Neurotoxicol Teratol. 2006; 28:536–547. [PubMed: 17067778]

DeFuria J, Shea TB. Arsenic inhibits neurofilament transport and induces perikaryal accumulation of phosphorylated neurofilaments: Roles of jnk and gsk-3beta. Brain Res. 2007; 1181:74–82. [PubMed: 17961518]

Franco JL, Posser T, Dunkley PR, Dickson PW, Mattos JJ, Martins R, et al. Methylmercury neurotoxicity is associated with inhibition of the antioxidant enzyme glutathione peroxidase. Free Radic Biol Med. 2009; 47:449–457. [PubMed: 19450679]

Franke TF, Yang SI, Chan TO, Datta K, Kazlauskas A, Morrison DK, et al. The protein kinase encoded by the akt proto-oncogene is a target of the pdgf-activated phosphatidylinositol 3-kinase. Cell. 1995; 81:727–736. [PubMed: 7774014]

Fretham SJ, Caito S, Martinez-Finley EJ, Aschner M. Mechanisms and modifiers of methylmercury-induced neurotoxicity. Toxicol Res (Camb). 2012; 1:32–38. [PubMed: 27795823]

Fujimura M, Usuki F. Low concentrations of methylmercury inhibit neural progenitor cell proliferation associated with up-regulation of glycogen synthase kinase 3beta and subsequent degradation of cyclin e in rats. Toxicol Appl Pharmacol. 2015; 288:19–25. [PubMed: 26184774]

Gao P, Li L, Ji L, Wei Y, Li H, Shang G, et al. Nrf2 ameliorates diabetic nephropathy progression by transcriptional repression of tgfbeta1 through interactions with c-jun and sp1. Biochim Biophys Acta. 2014; 1839:1110–1120. [PubMed: 25046864]

Gao Y, Howard A, Ban K, Chandra J. Oxidative stress promotes transcriptional up-regulation of fyn in bcr-abl1-expressing cells. J Biol Chem. 2009; 284:7114–7125. [PubMed: 19131339]

Grandjean P, Weihe P, White RF, Debes F, Araki S, Yokoyama K, et al. Cognitive deficit in 7-year-old children with prenatal exposure to methylmercury. Neurotoxicol Teratol. 1997; 19:417–428. [PubMed: 9392777]

Harada M. Minamata disease: Methylmercury poisoning in japan caused by environmental pollution. Crit Rev Toxicol. 1995; 25:1–24. [PubMed: 7734058]

Huang HC, Nguyen T, Pickett CB. Regulation of the antioxidant response element by protein kinase c-mediated phosphorylation of nf-e2-related factor 2. Proc Natl Acad Sci U S A. 2000; 97:12475–12480. [PubMed: 11035812]

Itoh K, Chiba T, Takahashi S, Ishii T, Igarashi K, Katoh Y, et al. An nrf2/small maf heterodimer mediates the induction of phase ii detoxifying enzyme genes through antioxidant response elements. Biochem Biophys Res Commun. 1997; 236:313–322. [PubMed: 9240432]

Itoh K, Wakabayashi N, Katoh Y, Ishii T, Igarashi K, Engel JD, et al. Keap1 represses nuclear activation of antioxidant responsive elements by nrf2 through binding to the amino-terminal neh2 domain. Genes Dev. 1999; 13:76–86. [PubMed: 9887101]

Jain AK, Jaiswal AK. Phosphorylation of tyrosine 568 controls nuclear export of nrf2. J Biol Chem. 2006; 281:12132–12142. [PubMed: 16513647]

Jain AK, Jaiswal AK. Gsk-3beta acts upstream of fyn kinase in regulation of nuclear export and degradation of nf-e2 related factor 2. J Biol Chem. 2007; 282:16502–16510. [PubMed: 17403689]

Kaspar JW, Jaiswal AK. Tyrosine phosphorylation controls nuclear export of fyn, allowing nrf2 activation of cytoprotective gene expression. FASEB J. 2011; 25:1076–1087. [PubMed: 21097520]

Kietzmann T, Samoylenko A, Immenschuh S. Transcriptional regulation of heme oxygenase-1 gene expression by map kinases of the jnk and p38 pathways in primary cultures of rat hepatocytes. J Biol Chem. 2003; 278:17927–17936. [PubMed: 12637567]

Kobayashi A, Kang MI, Okawa H, Ohtsuji M, Zenke Y, Chiba T, et al. Oxidative stress sensor keap1 functions as an adaptor for cul3-based e3 ligase to regulate proteasomal degradation of nrf2. Mol Cell Biol. 2004; 24:7130–7139. [PubMed: 15282312]

Li Z, Dong T, Proschel C, Noble M. Chemically diverse toxicants converge on fyn and c-cbl to disrupt precursor cell function. PLoS Biol. 2007; 5:e35. [PubMed: 17298174]

Lin CC, Yang CC, Chen YW, Hsiao LD, Yang CM. Arachidonic acid induces are/nrf2-dependent heme oxygenase-1 transcription in rat brain astrocytes. Mol Neurobiol. 2017; doi: 10.1007/s12035-017-0590-7

Lin HH, Lai SC, Chau LY. Heme oxygenase-1/carbon monoxide induces vascular endothelial growth factor expression via p38 kinase-dependent activation of sp1. J Biol Chem. 2011; 286:3829–3838. [PubMed: 21115498]

Livak KJ, Schmittgen TD. Analysis of relative gene expression data using real-time quantitative pcr and the 2(-delta delta c(t)) method. Methods. 2001; 25:402–408. [PubMed: 11846609]

Martin D, Rojo AI, Salinas M, Diaz R, Gallardo G, Alam J, et al. Regulation of heme oxygenase-1 expression through the phosphatidylinositol 3-kinase/akt pathway and the nrf2 transcription factor in response to the antioxidant phytochemical carnosol. J Biol Chem. 2004; 279:8919–8929. [PubMed: 14688281]

Newland MC, Reile PA. Blood and brain mercury levels after chronic gestational exposure to methylmercury in rats. Toxicol Sci. 1999; 50:106–116. [PubMed: 10445759]

Ni M, Li X, Yin Z, Sidoryk-Wegrzynowicz M, Jiang H, Farina M, et al. Comparative study on the response of rat primary astrocytes and microglia to methylmercury toxicity. Glia. 2011; 59:810–820. [PubMed: 21351162]

Pronk TE, van der Veen JW, Vandebriel RJ, van Loveren H, de Vink EP, Pennings JL. Comparison of the molecular topologies of stress-activated transcription factors hsf1, ap-1, nrf2, and nf-kappab in their induction kinetics of hmox1. Biosystems. 2014; 124:75–85. [PubMed: 25199502]

Sanguinetti AR, Cao H, Corley Mastick C. Fyn is required for oxidative- and hyperosmotic-stress-induced tyrosine phosphorylation of caveolin-1. Biochem J. 2003; 376:159–168. [PubMed: 12921535]

Shanker G, Mutkus LA, Walker SJ, Aschner M. Methylmercury enhances arachidonic acid release and cytosolic phospholipase a2 expression in primary cultures of neonatal astrocytes. Brain Res Mol Brain Res. 2002; 106:1–11. [PubMed: 12393259]

Shanker G, Aschner JL, Syversen T, Aschner M. Free radical formation in cerebral cortical astrocytes in culture induced by methylmercury. Brain Res Mol Brain Res. 2004; 128:48–57. [PubMed: 15337317]

Wang L, Jiang H, Yin Z, Aschner M, Cai J. Methylmercury toxicity and nrf2-dependent detoxification in astrocytes. Toxicol Sci. 2009; 107:135–143. [PubMed: 18815141]

Wang SH, Shih YL, Kuo TC, Ko WC, Shih CM. Cadmium toxicity toward autophagy through ros-activated gsk-3beta in mesangial cells. Toxicol Sci. 2009; 108:124–131. [PubMed: 19126599]

Yadav V, Denning MF. Fyn is induced by ras/pi3k/akt signaling and is required for enhanced invasion/migration. Mol Carcinog. 2011; 50:346–352. [PubMed: 21480388]

Yin Z, Milatovic D, Aschner JL, Syversen T, Rocha JB, Souza DO, et al. Methylmercury induces oxidative injury, alterations in permeability and glutamine transport in cultured astrocytes. Brain Res. 2007; 1131:1–10. [PubMed: 17182013]

Yin Z, Lee E, Ni M, Jiang H, Milatovic D, Rongzhu L, et al. Methylmercury-induced alterations in astrocyte functions are attenuated by ebselen. Neurotoxicology. 2011; 32:291–299. [PubMed: 21300091]

Yu R, Mandlekar S, Lei W, Fahl WE, Tan TH, Kong AN. P38 mitogen-activated protein kinase negatively regulates the induction of phase ii drug-metabolizing enzymes that detoxify carcinogens. J Biol Chem. 2000; 275:2322–2327. [PubMed: 10644681]

Highlights

- Astrocytes are vulnerable to MeHg-induced toxicity
- Methylmercury induces oxidative stress and Nrf2 activation
- Nrf2 translocates to the nucleus in response to methylmercury exposure
- Methylmercury exposure downregulates Fyn

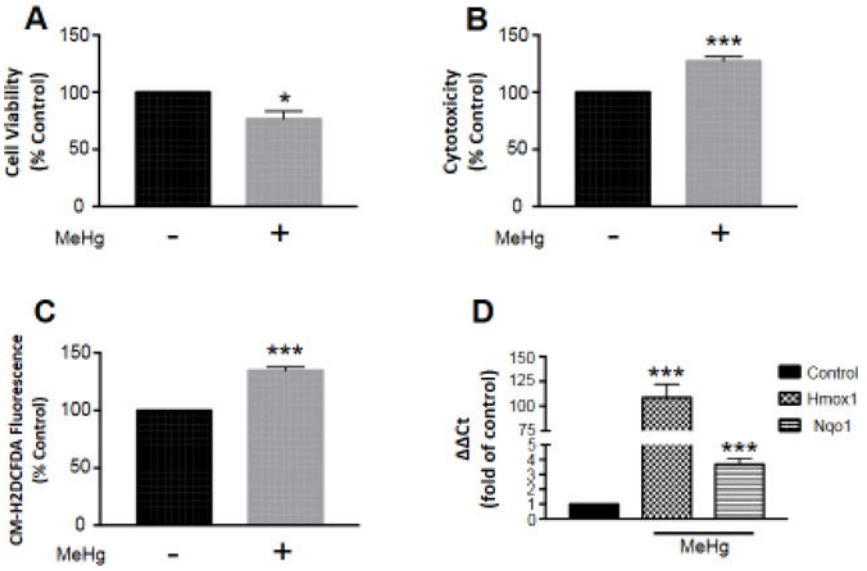

Figure 1.

MeHg-induced toxicity and oxidative stress are concomitant with Nrf2 activation of phase II detoxifying enzyme transcription. Astrocytes were treated with 5 μM MeHg for 6 hours, and cell viability (A; n =3) and cytotoxicity (B; n = 4) assessed by MTT and LDH assays, respectively. ROS generation (C; n = 4) was also measured by CM-H2DCFDA fluorescence, to indicate oxidative stress. Further, Nrf2 activation was confirmed by qRT-PCR of target genes Hmox1 (n = 5) and Nqo1 (n =6) (D). All data were normalized to untreated controls, and represent the mean ± SEM. *$p < 0.05$, ***$p < 0.001$

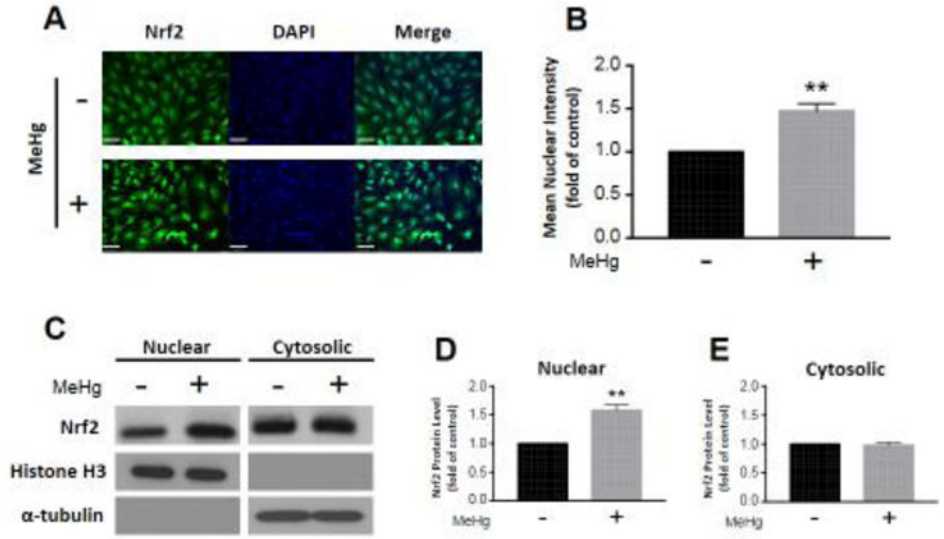

Figure 2.

Nrf2 translocates to the nucleus in response to MeHg exposure. Astrocytes were treated with 5 μM MeHg for 6 hours, and immunostained for Nrf2 (A). Nrf2 mean intensity in cell nuclei was quantified from four distinct images (B; n = 4). Further, Nrf2 protein level was measured in nuclear (C,D; n = 3) and cytosolic fractions (C,E; n = 3) separated by subcellular fractionation. Representative blots for nuclear and cytosolic Nrf2, histone H3, and α-tubulin are displayed (C). Nuclear and cytosolic fractions were normalized to histone H3 and α-tubulin, respectively. All data were normalized to untreated controls, and represent the mean ± SEM. **p < 0.01, scale bar = 60 μm

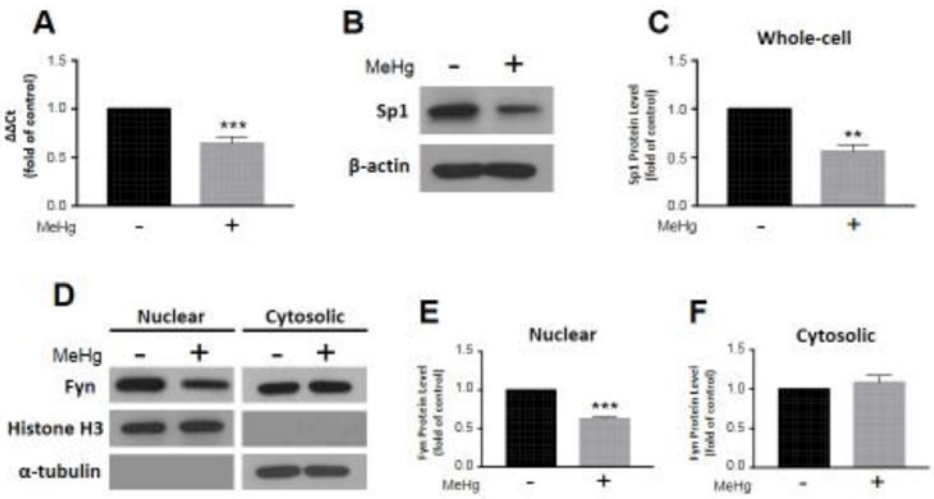

Figure 3.

Fyn expression and nuclear localization diminish consequent to MeHg exposure. Astrocytes were treated with 5 μM MeHg for 6 hours, and Fyn transcription (A; n = 6) assessed by qRT-PCR. Sp1 protein level was measured in whole-cell lysates, and normalized to β-actin (B,C; n = 3). Representative blots for Sp1 and β-actin are displayed (B). Further, Fyn protein level was quantified in nuclear (D,E; n = 3) and cytosolic fractions (D,F; n = 3) separated by subcellular fractionation. Representative blots for nuclear and cytosolic Fyn, histone H3, and α-tubulin are displayed (D). Nuclear and cytosolic fractions were normalized to histone H3 and α-tubulin, respectively. All data were normalized to untreated controls, and represent the mean ± SEM. **$p < 0.01$, ***$p < 0.001$

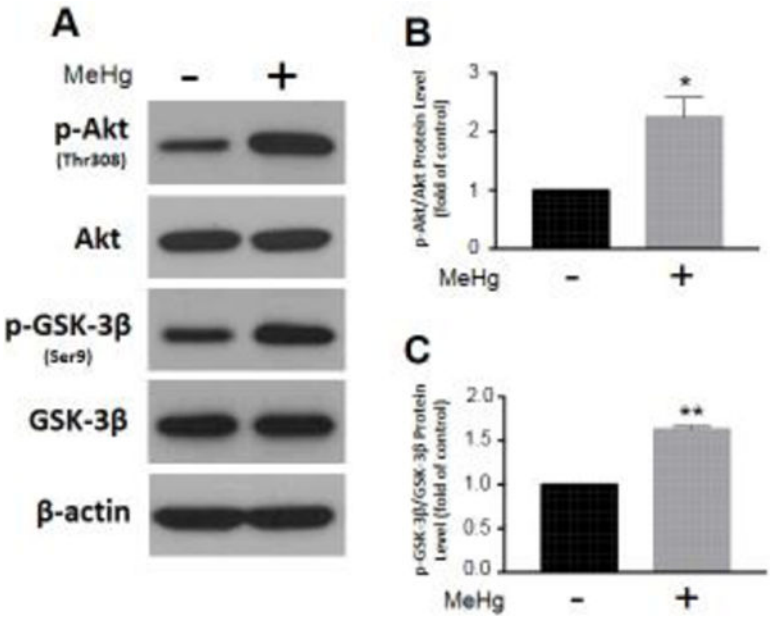

Figure 4.

MeHg exposure alters the Akt/GSK-3β signaling pathway, which regulates Fyn nuclear import. Astrocytes were treated with 5 μM MeHg for 6 hours, and relevant protein levels assessed by whole-cell western blot. Representative blots for p-Akt(Thr308), Akt, p-GSK-3β(Ser9), GSK-3β, and β-actin are displayed (A). p-Akt (B; n = 3) and p-GSK-3β (C; n = 3) were normalized to total Akt and GSK-3β, respectively. All data were normalized to untreated controls, and represent the mean ± SEM. *$p < 0.05$, **$p < 0.01$

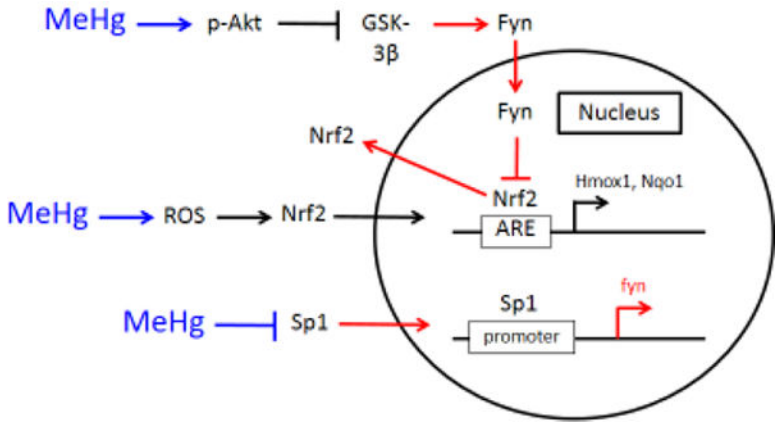

Figure 5.

MeHg augments Nrf2 activation by downregulation of the Src family kinase Fyn. MeHg activates Akt, which in turn inhibits GSK-3β. Thus, GSK-3β does not signal Fyn nuclear import. ROS generation consequent to MeHg exposure promotes Nrf2 nuclear localization, which upregulates Hmox1 and Nqo1 transcription. Further, MeHg reduces Sp1 protein, which results in decreased Fyn gene expression. Blue arrows indicate the effects of MeHg, while red arrows designate processes disrupted subsequent to MeHg exposure.